



The Breeding Sex Ratio Interacts With Demographic History to Shape Comparative Patterns of Variation on the X Chromosome and the Autosomes

William J. Spurley ^{1,*}, Bret A. Payseur ^{1,*}

¹Laboratory of Genetics, University of Wisconsin-Madison, Madison, WI, USA

*Corresponding authors: E-mails: wspurley@wisc.edu; bret.payseur@wisc.edu.

Accepted: February 25, 2025

Abstract

In many populations, unequal numbers of females and males reproduce each generation. This imbalance in the breeding sex ratio shapes patterns of genetic variation on the sex chromosomes and the autosomes in distinct ways. Despite recognition of this phenomenon, effects of the breeding sex ratio on some aspects of variation remain unclear, especially for populations with nonequilibrium demographic histories. To address this gap in the field, we used coalescent simulations to examine relative patterns of variation at X-linked loci and autosomal loci in populations spanning the range of breeding sex ratio with historical changes in population size. Shifts in breeding sex ratio away from 1:1 reduce nucleotide diversity and the number of unique haplotypes and increase linkage disequilibrium and the frequency of the most common haplotype, with contrasting effects on X-linked loci and autosomal loci. Strong population bottlenecks transform relationships among the breeding sex ratio, the site frequency spectrum, and linkage disequilibrium, while relationships among the breeding sex ratio, nucleotide diversity, and haplotype characteristics are broadly conserved. Our findings indicate that evolutionary interpretations of variation on the X chromosome should consider the combined effects of the breeding sex ratio and demographic history. The genomic signatures we report could be used to reconstruct these fundamental population parameters from genomic data in natural populations.

Key words: breeding sex ratio, X chromosome, population genomics, demographic history.

Significance

The breeding sex ratio is a fundamental evolutionary parameter, but genomic analyses routinely assume that it is 1:1. Our research characterizes the relationships between the breeding sex ratio and multiple facets of genomic variation and shows how these relationships change in the context of dynamic demographic histories. In doing so, we provide increasingly realistic expectations for patterns of X-linked and autosomal variation in population genomic datasets collected from natural populations.

Introduction

Dioecious organisms have two biological parents. Despite this fact, females and males can contribute unequally to the next generation from an evolutionary perspective. Polygyny (the mating of males with multiple females) biases the breeding sex ratio (BSR) away from 1:1 toward females,

whereas polyandry (the mating of females with multiple males) pushes the BSR toward males. Even in populations in which most members mate monogamously, extra-pair mating can distort the BSR away from 1:1 (Fernandez-Duque and Huck 2013; Huck et al. 2020). Sexual dimorphism in life-history traits, including

© The Author(s) 2025. Published by Oxford University Press on behalf of Society for Molecular Biology and Evolution.

This is an Open Access article distributed under the terms of the Creative Commons Attribution-NonCommercial License (<https://creativecommons.org/licenses/by-nc/4.0/>), which permits non-commercial re-use, distribution, and reproduction in any medium, provided the original work is properly cited. For commercial re-use, please contact reprints@oup.com for reprints and translation rights for reprints. All other permissions can be obtained through our RightsLink service via the Permissions link on the article page on our site—for further information please contact journals.permissions@oup.com.

generation time and lifespan, can also lead to unequal reproductive contributions by females and males (Lawler 2009; Amster and Sella 2020). Consequently, populations with BSRs that depart from 1:1 are expected to be common in nature.

Regardless of the cause of shifts in the BSR, this fundamental demographic parameter is predicted to leave signatures in genomic patterns of variation. The BSR shapes the effective population size (N_e), which captures the effects of genetic drift and is a key determinant of genetic variation (Wright 1940; Kimura and Crow 1963; Waples 2022). At autosomal loci, N_e is reduced as the BSR moves away from 1:1 (Hill 1972; Crow and Denniston 1988). The decline in N_e is symmetrical because a male bias (a higher proportion of breeding males in the population) and a female bias (a higher proportion of breeding females in the population) both decrease the number of unique autosomes contributing to the next generation (Caballero 1995).

The effects of the BSR on sex-linked loci are distinct from those on autosomal loci because the sex chromosomes are inherited differently. In species with X/Y chromosomal sex determination, the N_e of nonrecombining Y-linked loci reflects the number of unique breeding males in the population. When the BSR is 1:1 in a population of constant size, the N_e of Y-linked loci is expected to be $\frac{1}{4}$ the N_e of autosomal loci (Caballero 1995). A female bias in the BSR shifts the ratio of N_e for Y-linked loci and autosomal loci below $\frac{1}{4}$, while a male bias moves the ratio above $\frac{1}{4}$ (Wright 1933). The relationship between X-linked loci and the BSR is more complex. Due to hemizyosity of the X chromosome in males, the N_e of X-linked loci is expected to be $\frac{3}{4}$ the N_e of autosomal loci in a population of constant size (Wright 1933; Hill 1972). When the BSR is biased toward males, there are fewer total copies of the X chromosome in the breeding population, and the N_e of X-linked loci is lower than $\frac{3}{4}$ the N_e of autosomal loci (Caballero 1995). As the BSR shifts away from 1:1 in favor of females, the N_e for X-linked loci becomes more similar to the N_e of autosomal loci and even exceeds it at extreme female biases (Caballero 1995; Musharoff et al. 2019). Expectations are reversed for species with ZW sex chromosomes, where females are the heterogametic sex.

The effects of the BSR on N_e provide a straightforward path to understanding the connection between the BSR and patterns of genetic variation. The population mutation rate (θ), a primary determinant of levels of genetic variation under neutrality, is a product of N_e and the per-site, per-generation mutation rate (Watterson 1975). The population recombination rate (ρ), a primary determinant of linkage disequilibrium (LD) and haplotype structure, is a product of N_e and the per-site, per-generation recombination rate (Hill 1981; Hudson 1987). Changes in the BSR alter these parameters in different ways for X-linked loci and autosomal loci. For example, a male bias disproportionately

reduces N_e , and thus θ , at X-linked loci relative to autosomal loci, with concomitant effects on nucleotide diversity (Charlesworth 2001). A male bias differentially inflates LD at X-linked loci compared with autosomal loci because two factors decrease ρ : reduced N_e and a lack of recombination in males (Labuda et al. 2010; Lohmueller et al. 2010). The disparate effects of the BSR on patterns of genetic variation at X-linked loci and autosomal loci enable departures from a 1:1 BSR to be detected from population genomic data. Nucleotide diversity, the site frequency spectrum (SFS), and LD point to female biases in human populations (Hammer et al. 2008; Emery et al. 2010; Labuda et al. 2010; Musharoff et al. 2019).

Patterns of variation at X-linked loci and autosomal loci can also deviate from neutral expectations due to demographic history. A reduction in population size initially decreases X-linked diversity more substantially than autosomal diversity (Pool and Nielsen 2007). However, when the population size increases again, as in the case of a population bottleneck, X-linked diversity recovers to its original level faster than autosomal diversity (Pool and Nielsen 2007). Established effects of demographic history on the SFS (Tajima 1989; Griffiths and Tavaré 1998; Gutenkunst et al. 2009), LD (Waples 2006; Santiago et al. 2020), and haplotype structure (Lohmueller et al. 2009; Palamara et al. 2012) raise the prospect that these metrics could also differ between X-linked loci and autosomal loci when population size fluctuates (Wall et al. 2002).

Although departures from a 1:1 BSR are expected to be common in natural populations, gaps persist in our understanding of how this fundamental reproductive parameter shapes patterns of genetic variation. Importantly, little is known about how the BSR and demographic history *jointly* affect X-linked diversity and autosomal diversity (Webster and Wilson Sayres 2016; Musharoff et al. 2019). Moreover, theoretical and empirical studies connecting the BSR to genetic variation have focused on levels of diversity (Hammer et al. 2008; Emery et al. 2010; Clemente et al. 2018; Musharoff et al. 2019); expectations for measures of LD and haplotype structure remain unclear. To address these challenges, we examine the role of BSR in shaping variation at X-linked loci and autosomal loci in the context of realistic features of demographic history.

Results

To understand the joint effects of the BSR and demographic history on genomic patterns of sequence variation, we performed independent coalescent simulations of 1,000 unlinked loci on the X chromosome and 1,000 unlinked loci on the autosomes. We measured patterns of variation using a suite of common summary statistics that collectively capture levels of diversity, the SFS of polymorphisms, haplotype structure, and LD. To illustrate how the BSR interacts

with characteristics of demographic history to distort patterns of variation observed at mutation–recombination–drift equilibrium, we examined population bottlenecks with three different strengths, durations, and timings across the spectrum of BSR. Results for a wider range of scenarios are presented in the [Supplementary Material](#).

Effects of the BSR on Patterns of Variation at Mutation–Recombination–Drift Equilibrium

To first establish how the BSR alone affects variation on X-linked loci and autosomal loci, we focused on sex biases in the absence of demographic change. Relationships between the BSR and both nucleotide diversity (π) and Watterson's θ have been noted previously; we reintroduce them here to provide immediate comparison with scenarios in which both sex biases and demographic change are present (and to validate our simulation framework).

Average π (Fig. 1a) across autosomal loci and across X-linked loci recaptures established trends (Charlesworth 2001; Musharoff et al. 2019). For autosomal loci, π declines symmetrically with distance from a maximum at a proportion of females in the breeding population (p_f) = 0.5 (a 1:1 BSR). Alternatively, for X-linked loci, π is maximized with a slight female bias and declines similarly to the autosomal scenario as the BSR shifts away from this point. X-linked and autosomal diversity are similar at more extreme sex biases, particularly with a female bias. For both X-linked and autosomal loci, reductions in nucleotide

diversity directly mirror reductions in N_e that result from changes in the BSR (Caballero 1995). These patterns apply equally to Watterson's θ (Fig. 1b), resulting in no change in Tajima's D across all BSRs (Fig. 1c). Tajima's D , which is computed as the normalized difference between π and Watterson's θ , measures the skew in the SFS. Negative values indicate an enrichment of rare alleles (as can occur with a population expansion), while positive values indicate an enrichment of intermediate-frequency alleles (as can occur with a population bottleneck).

Effects of the BSR extend to summary statistics that capture haplotypes and LD. The average number of unique haplotypes across autosomal loci declines with stronger sex biases in each direction (Fig. 1d). For X-linked loci, the average number of unique haplotypes is maximized at a slight female bias. Although these trends resemble patterns for π and Watterson's θ , the number of haplotypes decays more slowly than π as the BSR moves away from 0.5. For X-linked loci, the frequency of the most common haplotype is maximized at extreme male bias, when the number of haplotypes is minimized (Fig. 1e). The squared correlation coefficient between allelic values, r^2 (averaged across pairs of single nucleotide polymorphisms), is higher for autosomal loci at extreme BSRs (Fig. 1f). For X-linked loci, r^2 is maximized at an extreme male bias and minimized at a slight female bias.

The interlocus variance of each summary statistic is also responsive to changes in the BSR ([supplementary fig. S1, Supplementary Material online](#)). The variance of π and the

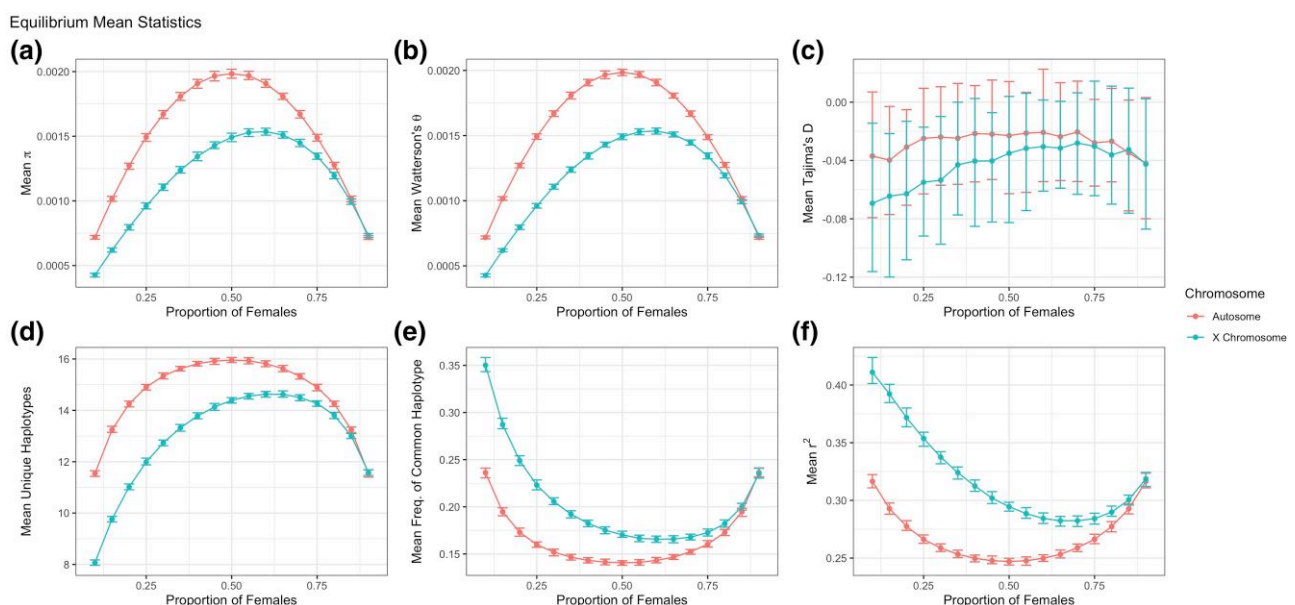


Fig. 1. Patterns of variation are sensitive to the BSR. a) Mean π , b) Watterson's θ , c) Tajima's D , d) number of haplotypes, e) frequency of the common haplotype, and f) r^2 under a constant population size at varying BSRs. Points represent mean values across 100 evolutionary replicates of 1,000 independent loci for X-linked loci (blue) and autosomal loci (red). Error bars summarize the 95% confidence interval by taking the 97.5th and 2.5th quantiles of each distribution of replicates.

variance of Watterson's θ follow patterns for the averages of these statistics described above. In contrast to average Tajima's D , the variance of Tajima's D is affected by changes in the BSR, with elevated variance at stronger sex biases. The frequency of the most common haplotype and r^2 also follow this pattern, but with less change across moderate BSR values. The variance in the number of haplotypes generally increases with the degree of sex bias, except for X-linked loci at the strongest male bias ($p_f = 0.1$).

Effects of the BSR and Bottleneck Strength on Patterns of Variation

To determine how the BSR interacts with demographic history to shape patterns of variation, we examined three different bottleneck strengths: a 50% reduction, an 80% reduction, and a 95% reduction from the ancestral size. For results reported in this section, we held duration and timing constant: bottlenecks lasted 500 generations and ended 500 generations ago.

Under a bottleneck, the relationships between the BSR and average levels of variation (π and Watterson's θ) for X-linked loci and autosomal loci resemble those in constant-size populations (Fig. 2a and b). For stronger bottlenecks, Watterson's θ is reduced more than π , particularly at moderate sex biases, which induces a dependence of Tajima's D on the BSR (Fig. 2c). At an 80% reduction, average Tajima's D begins to differentiate at strong male biases, but not at any other BSR. At a 95% reduction, Tajima's D is fully sensitive to the BSR: extreme sex biases confer

negative Tajima's D values, whereas moderate sex biases yield positive values.

As bottleneck strength increases, the number of unique haplotypes declines, and the frequency of the most common haplotype increases (Fig. 2d and e). Still, relationships between the BSR and haplotype patterns with a bottleneck resemble those in populations of constant size.

LD shows a distinct pattern. As bottlenecks increase in strength, average r^2 changes with the BSR in ways that depart from equilibrium patterns (Fig. 2f). With 50% and 80% reductions in population size, r^2 is elevated across most of the range of BSR, compared with equilibrium values. In contrast, a 95% reduction in population size transforms the relationship of the BSR and LD. In a surprising reversal of equilibrium patterns, r^2 is higher at autosomal loci than at X-linked loci when male bias is extreme. LD is also maximized for both X-linked loci and autosomal loci at moderate sex biases.

We considered the effects of bottleneck strength across additional scenarios of bottleneck timing and duration. Our results consistently indicate that changing bottleneck strength has no strong effect on relative patterns of X-linked loci and autosomal loci for π , Watterson's θ , and the haplotype summaries, regardless of bottleneck timing and duration. In contrast, bottlenecks shape the relationships among the BSR, Tajima's D , and r^2 in a manner that depends on each bottleneck parameter (supplementary figs. S2 and S3, Supplementary Material online). These findings demonstrate strong interactions between BSR and demographic history in determining the SFS and LD.

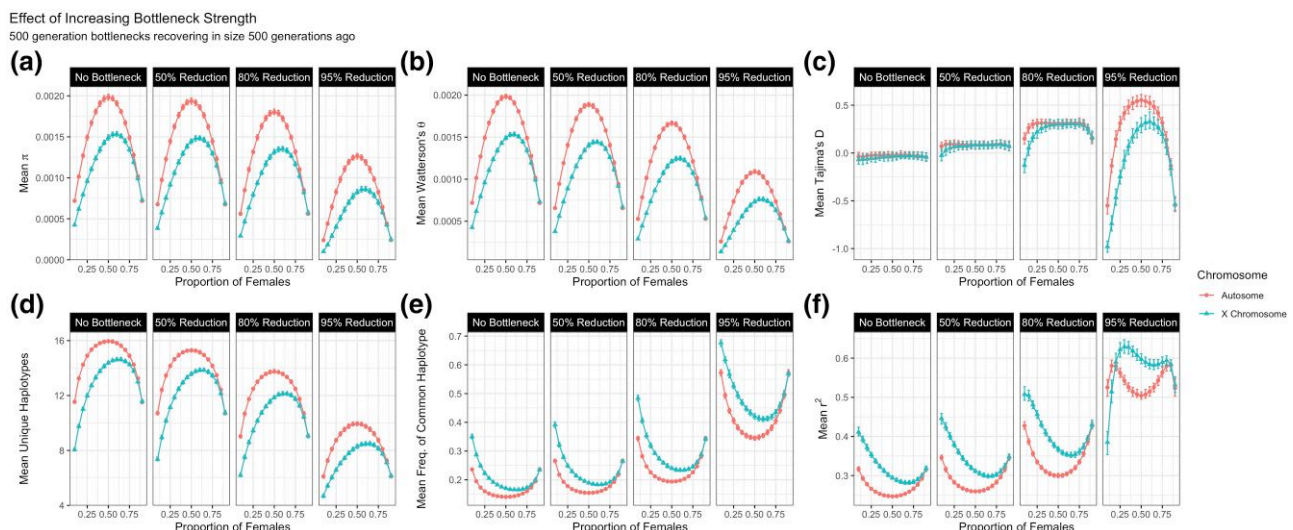


Fig. 2. Increasing population bottleneck strength changes the relationship between the BSR and patterns of variation. a) Mean π , b) Watterson's θ , c) Tajima's D , d) number of haplotypes, e) frequency of the common haplotype, and f) r^2 under bottlenecks with variable strength, lasting 500 generations, and recovering in size 500 generations ago. Points represent mean values across 100 evolutionary replicates of 1,000 independent loci for X-linked loci (blue triangles) and autosomal loci (red circles). Error bars summarize the 95% confidence interval by taking the 97.5th and 2.5th quantiles of each distribution of replicates. Each strength represents 50%, 80%, or 95% reduction from the ancestral population size (center left, center right, and right panels, respectively). The panels titled "No Bottleneck" represent simulations performed with a constant population size.

Increasing the strength of a bottleneck does not affect the relationship of the BSR with the interlocus variances of π or Watterson's θ and has little effect on the variances of r^2 and the frequency of the common haplotype (supplementary fig. S4, Supplementary Material online). In contrast, a 95% reduction in population size transforms the relationship between the variance of Tajima's D and the BSR, leaving a signature resembling mean r^2 at an 80% reduction (described above). The variance of the number of haplotypes is also sensitive to changes in bottleneck strength. With a weak bottleneck, the variance is greater for X-linked loci than autosomal loci (except when the male bias is extreme). As the strength of the bottleneck increases, the patterns of variance change among the moderate BSRs, leading to a higher variance in the haplotype count for autosomal loci than X-linked loci at a 95% reduction.

Effects of the BSR and Bottleneck Duration on Patterns of Variation

To explore how bottleneck duration affects relationships between BSR and patterns of variation, we simulated 100-generation, 500-generation, and 1,000-generation bottlenecks with a 95% reduction in size and a recovery 500 generations ago.

As bottleneck duration increases, average diversity is reduced, with relationships between the BSR and levels of variation mostly being maintained (Fig. 3a and b). These effects are only observed with strong bottlenecks; weaker

bottlenecks show little change in variation as duration increases (supplementary figs. S5 and S6, Supplementary Material online). Increasing bottleneck duration induces a strong dependence of BSR on Tajima's D with bottlenecks lasting 500 or 1,000 generations (Fig. 3c). With a 100-generation bottleneck, there is little differentiation of average Tajima's D at X-linked and autosomal loci except at an extreme male bias, where X-linked loci have a lower average value. For a 500-generation bottleneck, parabolic relationships emerge between the BSR and Tajima's D . For autosomal loci, Tajima's D is positive for all but the most extreme BSR values, whereas for X-linked loci, Tajima's D is negative at a wider range of BSRs. When the bottleneck lasts for 1,000 generations, Tajima's D for both X-linked and autosomal loci is shifted to be more negative.

Effects of the BSR on average haplotype number and average frequency of the most common haplotype do not change with bottleneck duration (Fig. 3d and e). In contrast, LD shows a different relationship to the BSR at each bottleneck duration (Fig. 3f). A 100-generation bottleneck leads to trends like those in the absence of a bottleneck, with average r^2 elevated throughout. A 500-generation bottleneck induces complex relationships between the BSR and r^2 that differ for strong and moderate sex biases (resembling the effects of a strong bottleneck, described above). At a 1,000-generation bottleneck, there is little differentiation between X-linked loci and autosomal loci at a female bias. For both classes of loci, a stronger sex bias confers reduced r^2 values, a stark contrast to the equilibrium scenario.

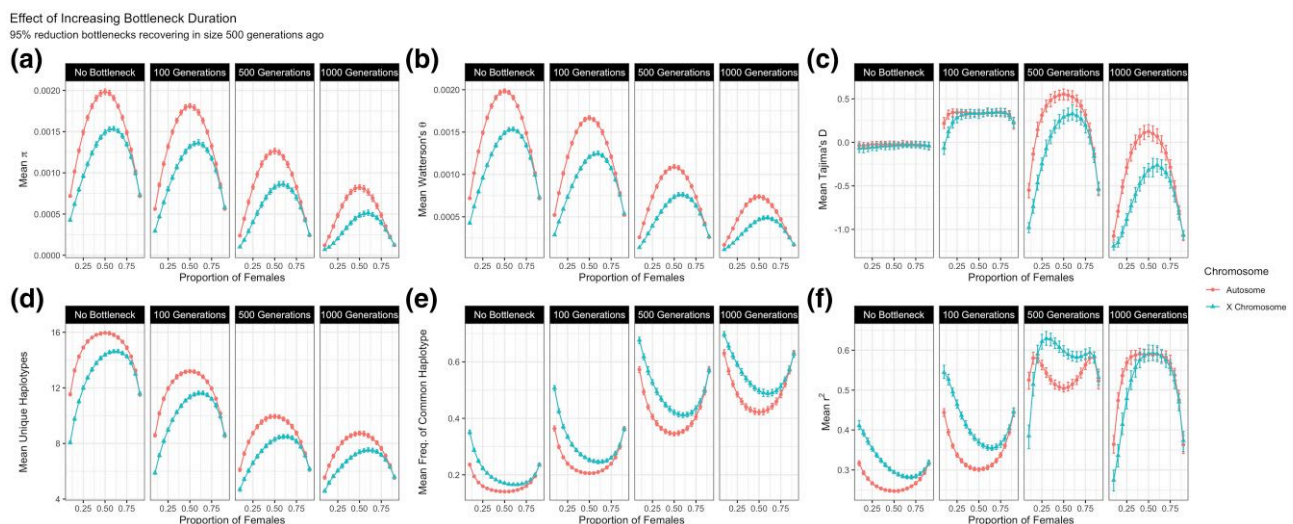


Fig. 3. Increasing bottleneck duration changes the relationship between the BSR and patterns of variation. a) Mean π , b) Watterson's θ , c) Tajima's D , d) number of haplotypes, e) frequency of the common haplotype, and f) r^2 under bottlenecks with variable duration, a 95% reduction, and recovering in size 500 generations ago. Points represent mean values across 100 evolutionary replicates of 1,000 independent loci for X-linked loci (blue triangles) and autosomal loci (red circles). Error bars summarize the 95% confidence interval by taking the 97.5th and 2.5th quantiles of each distribution of replicates. Each duration represents 100, 500, and 1,000 generation long bottlenecks (center left, center right, and right panels, respectively). The panels titled "No Bottleneck" represent simulations performed with a constant population size.

Relationships between the BSR and the interlocus variances of π and Watterson's θ are maintained as the duration of bottlenecks increases (supplementary fig. S7, Supplementary Material online). Nevertheless, the disparity between X-linked loci and autosomal loci is larger for longer bottlenecks. The variance of Tajima's D again takes on patterns resembling those for mean r^2 (see Fig. 3f). For both r^2 and the frequency of the most common haplotype, longer bottlenecks yield higher variances across the range of BSR, but there is a slight decline at the most extreme male bias. Variances in haplotype number are lower with extreme sex biases than at a balanced BSR.

Effects of the BSR and Bottleneck Timing on Patterns of Variation

To examine how changes in bottleneck timing affect the relationships between the BSR and patterns of variation, we simulated bottlenecks that recover to the original population size 500, 1,000, or 5,000 generations ago while holding constant the strength (95% reduction) and duration (500 generations).

More recent bottlenecks result in lower average diversity across the range of BSRs (Fig. 4a and 4b). With a bottleneck recovery 5,000 generations ago, there is little change in average Tajima's D with the BSR. In contrast, Tajima's D is dependent on the BSR when bottlenecks end 1,000 or 500 generations ago. A bottleneck recovering 500 generations ago yields more positive Tajima's D than a distant bottleneck at a moderate sex bias (Fig. 4c). Haplotype

summaries maintain their relationships with the BSR regardless of the timing of bottlenecks (Fig. 4d and e).

Varying bottleneck timing alters the relationship between the BSR and LD (Fig. 4f). When a bottleneck ends 5,000 generations ago, average r^2 at autosomal loci is largely unchanged across the range of BSRs. For X-linked loci, average r^2 is maximized at an extreme male bias and minimized at an extreme female bias. When a bottleneck ends 1,000 generations ago, autosomal r^2 is maximized at two points: a strong male bias ($p_f=0.2$) and a strong female bias ($p_f=0.8$). For X-linked loci, average r^2 increases from an extreme male bias to a moderate one ($p_f=0.1$ to 0.3), and then among the moderate sex biases ($p_f=0.3$ to 0.8), it decreases gradually, before rapidly decreasing at a strong female bias ($p_f=0.8$ to 0.9). Similar patterns emerge for a bottleneck ending 500 generations ago, but with a greater difference between X-linked loci and autosomal loci at moderate sex biases. The ability to distinguish the effect of changes in bottleneck timing on patterns of variation is reduced for weaker bottlenecks (supplementary fig. S8, Supplementary Material online).

Although the timing of bottlenecks has little effect on the interlocus variance of π and the variance of Watterson's θ , the variance of Tajima's D responds to changes in timing in patterns that resemble the average r^2 (supplementary fig. S9, Supplementary Material online). The variance of the number of haplotypes is more sensitive to changes in bottleneck timing at moderate sex biases compared with extreme sex biases. For the frequency of the most common haplotype and r^2 , more recent

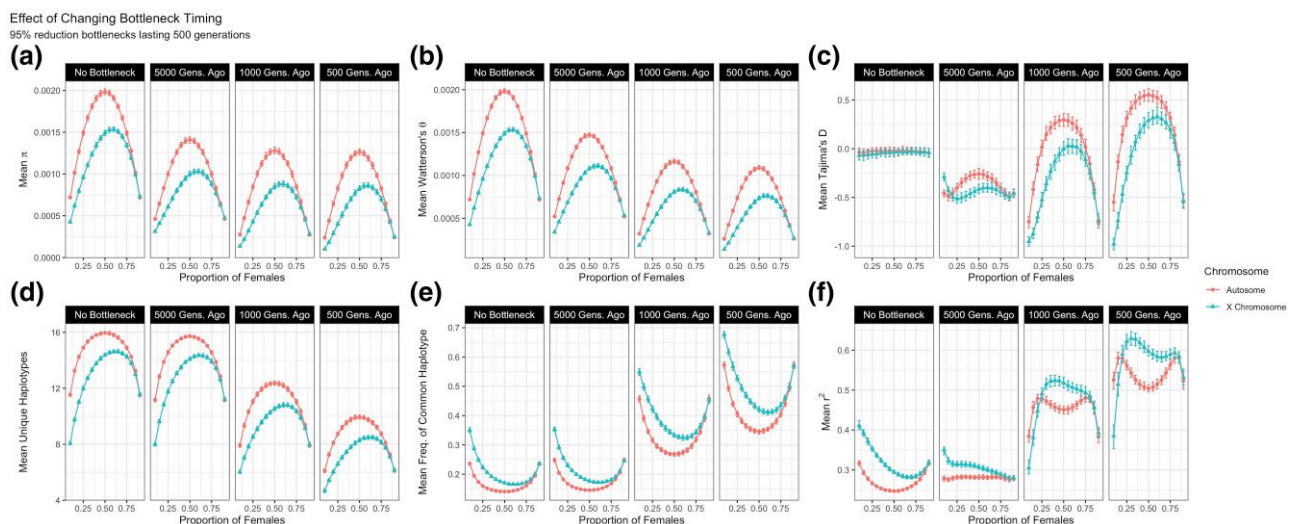


Fig. 4. The timing of a bottleneck influences the relationship between the BSR and patterns of variation. a) Mean π , b) Watterson's θ , c) Tajima's D , d) number of haplotypes, e) frequency of the common haplotype, and f) r^2 under bottlenecks with variable timing, a 95% reduction, and lasting 500 generations. Points represent mean values across 100 evolutionary replicates of 1,000 independent loci for X-linked loci (blue triangles) and autosomal loci (red circles). Error bars summarize the 95% confidence interval by taking the 97.5th and 2.5th quantiles of each distribution of replicates. Each timing represents bottlenecks recovering to the ancestral population size 5000, 1000, and 500 generations ago (center left, center right, and right panels, respectively). The panels titled "No Bottleneck" represent simulations performed with a constant population size.

bottlenecks lead to elevated variances, but less so for an extreme male bias.

Effects of the BSR and Population Expansions on Patterns of Variation

To perform an initial investigation into how patterns of variation are jointly influenced by the BSR and population growth, we simulated populations expanding at an exponential rate to ten times their ancestral size. The first set of simulations modeled a population experiencing growth for 460 generations at an exponential rate of 0.005. The second set of simulations modeled a population experiencing growth for 46 generations at an exponential rate of 0.05. The longer and slower expansion confers slightly larger differences from equilibrium values of summary statistics than the shorter and faster expansion ([supplementary fig. S10, Supplementary Material online](#)). For π , Watterson's θ , and the two haplotype statistics, the effect of the BSR on X-linked and autosomal loci is largely conserved, with expansions resulting in higher diversity and more haplotypes. In contrast to results for population bottlenecks, Tajima's D and r^2 show no evidence of interactions between the BSR and population expansions. Tajima's D at X-linked and autosomal loci is sensitive to changes in the BSR in expanding populations, but these patterns are consistent across the conditions we explored ([supplementary fig. S10c, Supplementary Material online](#)).

Investigating Patterns of Variation Sensitive to Interactions Between BSR and Demographic History

To further investigate interactions between the BSR and demographic history, we examined the SFS and LD in greater detail. First, we compared the full SFS (of which Tajima's D is a summary) for X-linked loci and autosomal loci in a population with a severe bottleneck (95% strength, lasting 500 generations, and recovering 500 generations ago) and in a population of constant size, each across a range of BSR values. Without changes in population size, the average SFS is the same in populations with different BSR values, as the proportion of SNPs in each frequency bin is independent of N_e (Fu 1995; [supplementary fig. S11, Supplementary Material online](#)). With a bottleneck and no sex bias ($p_f = 0.5$), the proportion of alleles with intermediate frequencies increases, but more noticeably for the autosomes ([supplementary fig. S12, Supplementary Material online](#)). This pattern aligns with the positive values for Tajima's D observed for this demographic history and BSR (see Fig. 2c, middle right panel). With a bottleneck, the proportion of singletons increases with either male bias or female bias. This increase in singletons, which confers negative values of Tajima's D , marks a shift in abundance toward more recent mutations. With the loss of diversity caused by reductions in N_e from both a strong sex bias and a bottleneck,

a larger share of variants emerge after the recovery to the ancestral population size. As a result, the shape of the SFS and negative values of Tajima's D reflect a population expansion.

To begin to explore explanations for unusual patterns of LD, we considered the scenario of a strong bottleneck (95% reduction in size, lasting 500 generations, and recovering 500 generations ago) and a strong male bias ($p_f = 0.1$; Fig. 4f, middle right panel). In this case, we observe two distinct peaks in the r^2 distribution around values of 0.1 and 0.9 for X-linked loci ([supplementary fig. S13, Supplementary Material online](#), top right panel). A preliminary examination of genealogies at 1,000 X-linked loci simulated under this scenario shows that samples at loci with $r^2 < 0.1$ have an average time to the most recent common ancestor (TMRCA) of 906 generations ([supplementary fig. S13, Supplementary Material online](#), bottom right panels), which occurs during the epoch of reduced N_e . This subset of loci effectively experiences a population expansion, leading to very low LD. In contrast, samples at loci with $r^2 > 0.9$ have an average TMRCA of 5,090 generations ([supplementary fig. S12, Supplementary Material online](#), bottom right panels), which long precedes the reduction in N_e . This subset of loci experiences the full bottleneck, which elevates LD. Although this explanation is preliminary, it suggests that deeper inspection of genealogical properties will be required to fully elucidate the patterns of variation we report.

Effects of the BSR and Sex Differences in Mutation Rate on Patterns of Variation

To explore the capacity for sex-biased mutation to jointly shape patterns of variation with BSR and demographic history, we simulated the same scenarios described above, but with a male mutation rate three times the female mutation rate ([supplementary fig. S14, Supplementary Material online](#)). As expected, patterns of variation at autosomal loci are unaffected by this change. Additionally, r^2 is unaltered for both X-linked loci and autosomal loci. At X-linked loci, π , Watterson's θ , and the number of unique haplotypes are reduced by male-biased mutation, and the frequency of the most common haplotype increases. Effects are less severe for the two haplotype summaries than for π and Watterson's θ . Similar patterns are observed with population bottlenecks, suggesting little interaction between sex differences in mutation rate and demographic history ([supplementary fig. S15, Supplementary Material online](#)).

Discussion

From a genetic perspective, the X chromosome is special. Unequal transmission between the sexes and alternating ploidy between haploid males and diploid females make it difficult to interpret patterns of variation on the X

chromosome compared to autosomes (Hudson and Turelli 2003; Kirkpatrick et al. 2010). Partly because of these complications, the X chromosome is often ignored in population genomic studies. However, the biological factors that make the X chromosome difficult to compare with the autosomes also predict unique evolutionary dynamics. For example, the X chromosome offers the capacity to reveal differences between the sexes in the operation of evolutionary processes, including natural selection (Corl and Ellegren 2012) and migration (Goldberg and Rosenberg 2015).

The BSR must be considered when drawing evolutionary inferences from relative patterns of variation on the X chromosome and the autosomes. Our results confirm and extend this notion in two principal ways, illustrating the genomic consequences of the BSR for empirical datasets. First, we characterize the effects of the BSR across multiple axes of variation, providing a fuller picture of the genomic signatures of this fundamental reproductive parameter. Second, we distinguish facets of variation shaped by interactions between the BSR and demographic history (LD and SFS) from those for which relationships with the BSR are more stable (nucleotide diversity and haplotype characteristics).

Our conclusions are tempered by limitations of our study design. The approach we used to demonstrate the effects of the BSR on patterns of variation strictly applies to species that utilize sex chromosomes for sex determination. Our coalescent simulations modeled the BSR and demographic parameters through their effects on N_e rather than modeling a specific mating structure. Although our simulations considered a broad range of BSRs, we examined a small subset of parameter values for demographic events, particularly for population expansions. Further exploration of population size changes and other demographic scenarios may reveal new interactions between the BSR and demographic history. We stipulated constancy of the BSR throughout population history, even as we might expect this parameter to shift over time due to changes in mating behavior and life-history traits. Finally, we assumed that all loci evolve neutrally. We sought to mimic a population genomic study that prioritizes intergenic loci far from genes for demographic inference, but isolating loci that evolve neutrally can be a challenge.

Despite these caveats, our findings are relevant to topical challenges in empirical population genomics, including the role of linked selection in shaping genomic patterns of variation. Beneficial mutations that arise on the X chromosome enjoy shorter sojourn times, regardless of dominance (Avery 1984). Recessive, X-linked beneficial mutations also fix faster than their autosomal counterparts (Charlesworth et al. 1987), and the dominance conditions for faster X evolution are less restrictive when the BSR is female biased (Laporte and Charlesworth 2002; Vicoso and Charlesworth 2009). Together, these factors predict

reduced X-linked diversity compared with autosomal diversity (Begun and Whitley 2000; Betancourt et al. 2004). In contrast, quicker removal of recessive, X-linked deleterious mutations exposed in males leaves a larger proportion of neutral variants unlinked to deleterious mutations, predicting higher diversity on the X chromosome under background selection (Charlesworth et al. 1993; Aquadro et al. 1994; Charlesworth 1996). Our results should motivate broader incorporation of the BSR alongside demographic history into models of selection used to predict X-linked variation, including levels of diversity, the SFS, LD, and haplotype patterns (Veeramah et al. 2014; Harris et al. 2024).

Our findings hold special implications for demographic inferences drawn from genomic patterns of variation. The SFS is commonly used to reconstruct historical population sizes (e.g. Gutenkunst et al. 2009), but estimates may be biased by unmodeled departures from a 1:1 BSR. As an instructive example, consider the SFS in a population with a 95% size reduction lasting 1,000 generations that recovers in size 500 generations ago (Fig. 4c, right panel). If the BSR is sufficiently female biased ($p_f > 0.6$), Tajima's D for autosomal loci is more negative than expected when the BSR is balanced. The higher proportion of singletons driving this pattern could be misconstrued as solely due to demographic history if the BSR is not considered. Methods of demographic inference based on LD may also be biased if they fail to account for the BSR. For example, recent changes in N_e can be reconstructed from LD between loci spaced at variable genetic distances (Santiago et al. 2020). In our simulations of recent, strong bottlenecks, marked sex biases ($p_f > 0.8$ or $p_f < 0.3$) produced lower values of r^2 , which could be misinterpreted as decreases in LD caused by increases in N_e . Overall, our results suggest that the mischaracterization of demographic history is more likely when populations experience strong bottlenecks. To minimize these complications, we encourage the continued development of methods with the capacity for joint estimation of the BSR and demographic history (Clemente et al. 2018; Musharoff et al. 2019).

Knowledge of the BSR can improve inferences about demographic history and selection, and comparisons between the X chromosome and the autosomes make it possible to estimate this parameter from population genomic data. Building on earlier rejections of a balanced BSR in humans based on individual summary statistics (Hammer et al. 2008; Keinan et al. 2009; Emery et al. 2010), methods have been developed to estimate the BSR using maximum likelihood analysis of the SFS (Musharoff et al. 2019) and Bayesian analysis of multipopulation genealogies (Clemente et al. 2018). The effects of the BSR we report could stimulate the creation of methods that jointly consider multiple facets of variation to estimate the BSR using composite likelihood or approximate Bayesian

computation. Comparison of BSR estimates across a diverse collection of populations and species could point to biological drivers of this fundamental reproductive parameter.

Materials and Methods

Theoretical Approach to Simulate the BSR

To rapidly simulate datasets across a range of BSR values, we followed established theory connecting BSR with effective population size (N_e) (Caballero 1995; Musharoff et al. 2019). We calculated the N_e of an autosomal locus as:

$$N_e^A = 4p_f(1 - p_f)N_e, \quad (1)$$

where p_f is the proportion of breeding females in the population (N_f/N_e). We calculated the N_e of an X-linked locus as:

$$N_e^X = \frac{9p_f(1 - p_f)}{2(2 - p_f)} N_e. \quad (2)$$

These effective population sizes were used as input to coalescent simulations.

A Pipeline for Joint Simulation of the BSR and Demographic Change

To simulate the interaction of the BSR and demographic history, we developed a pipeline that utilizes coalescent

simulations from the package *msprime* v1.2.0 (Baumdicker et al. 2022). The process began by providing values of N_e , mutation rate, and recombination rate (Fig. 5). We specified an N_e of 10,000, a mutation rate of 5×10^{-8} (per-site, per-generation), and a recombination rate of 5×10^{-8} (per-site, per-generation) for the results shown. After specifying these parameters, both a demographic history and a BSR were applied. Using *msprime*'s demography objects, we constructed a population bottleneck with size changes specified at defined time points. We primarily focused our examination of demographic history on population bottlenecks because they are commonly experienced by natural populations and such changes are known to affect genomic patterns of variation.

After initializing a demographic history, we imposed a BSR on the population, using Equations (1) (autosomal loci) and (2) (X-linked loci) to adjust N_e for each epoch. To accommodate their need for separate adjustment of N_e , we simulated autosomal loci and X-linked loci independently. To account for effects of the BSR on the recombination rate at X-linked loci, we rescaled the recombination rate as:

$$c^X = \frac{2p_f}{1 + p_f} c \quad (3)$$

Where c is the original (per-site, per-generation) recombination rate and p_f is again the proportion of the breeding population that is female (Labuda et al. 2010; see Lohmueller et al. 2010). By adjusting the recombination

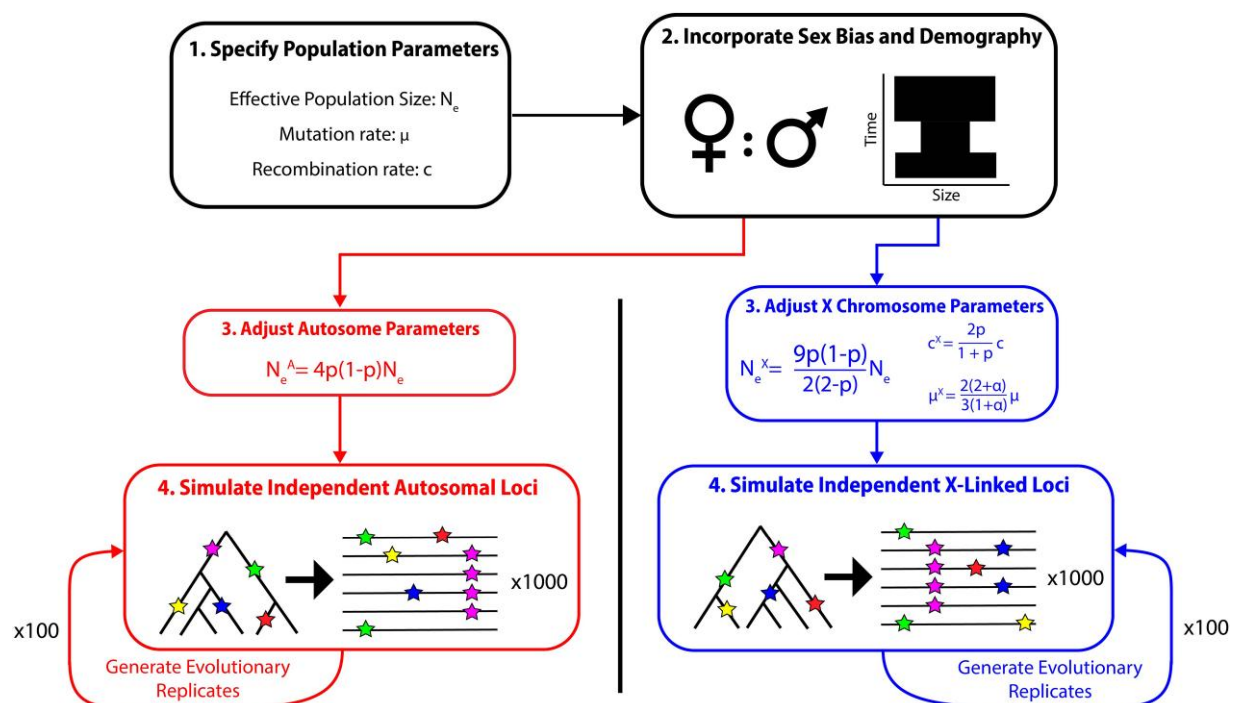


Fig. 5. Summary of simulation framework used for generating X-linked loci and autosomal loci for comparison under specified BSRs and demographic histories.

rate in this manner, we could capture the average behavior of X-linked loci without needing to simulate separate sexes. To account for the effects of sex differences in mutation rate, we rescaled the mutation rate at X-linked loci as:

$$\mu^X = \frac{2(2 + \alpha)}{3(1 + \alpha)}\mu, \quad (4)$$

Where μ is the (per-site, per-generation) mutation rate and $\alpha = \mu_M/\mu_F$ is the ratio of the male mutation rate and the female mutation rate (Miyata et al. 1987). For autosomal loci, mutation rates and recombination rates were unchanged.

After making the adjustments described above, we performed simulations with two levels of replication with the goal of mimicking genomic patterns of variation in population samples from natural populations. We first simulated X-linked loci and autosomal loci as 10 kb windows. For each window, *msprime* generated an independent genealogy and added mutations according to input parameters. For each window, we organized *msprime* output as a dataset of single nucleotide polymorphism (SNP) genotypes in variant call format for calculating population genetic summary statistics. All summary statistics were computed using the package *scikit-allel* v1.3.5 (<https://github.com/cggh/scikit-allel>). We used this process to simulate a genomic dataset composed of 1,000 X-linked loci and 1,000 autosomal loci. Genomic patterns of variation for this dataset were summarized using the mean and variance of each summary statistic taken separately across X-linked loci and across autosomal loci. For each combination of BSR and demographic parameters, we simulated 100 evolutionary replicates. We calculated the average of the mean and variance of each summary statistic across the 100 replicates, separately for X-linked loci and autosomal loci. These values were visualized, with the 2.5th and 97.5th quantiles of the distributions used as approximate confidence intervals across genomic datasets.

Quantifying Patterns of Variation

To capture the effects of the BSR and demographic history on genomic patterns of variation, we computed a suite of summary statistics. We calculated the average pairwise number of differences (Tajima 1983) and Watterson's θ to quantify levels of variation. We used Tajima's D (Tajima 1989) as a summary of the SFS of polymorphisms. We tabulated the number of unique haplotypes and the frequency of the most common haplotype as metrics of haplotype structure. We measured average pairwise r^2 (after removing singleton SNPs) (Hill and Robertson 1968) to describe LD. We treated phase as known.

Simulated Parameter Values

To determine how relationships between the BSR patterns of variation are affected by demographic history, we

simulated a range of population bottlenecks. All scenarios were simulated across a full range of BSR, starting with a proportion of females in the breeding population equal to 0.1 (10% female and 90% male) and increasing by 0.05 until ending at 0.9 (90% female and 10% male). Each bottleneck was modeled as an instantaneous reduction in N_e , a period at reduced N_e , and an instantaneous increase to return to the original N_e . For each of three bottleneck parameters—strength, timing, and duration—we specified three values. For bottleneck strength, we simulated 50%, 80%, and 95% reductions in N_e . For bottleneck timing, we simulated a size recovery occurring 500, 1,000, and 5,000 generations ago. For bottleneck duration, we simulated bottlenecks lasting 100, 500, and 1,000 generations. We simulated every combination of parameters, for a total of 27 unique bottlenecks.

To begin to explore an additional demographic model, we simulated two exponential population expansions across a full range of BSRs. The population expansions result in a contemporary size that is ten times larger than the ancestral size, with variable growth rates. Both expansions conclude 1,000 generations ago. The growth rates, g , defined as se^{-gt} with initial size s at time t in *msprime* (working backward in time), were 0.05 and 0.005 for these scenarios, resulting in doubling times of about 14 generations and 140 generations, respectively. The duration of each expansion was set such that the desired increase in size was achieved, 46 generations when $g=0.05$ and 460 generations when $g=0.005$.

We also considered how mutation rate and recombination rate affect the relationship between BSR and patterns of variation. We simulated the following scenarios. First, we specified mutation and recombination rates of 5×10^{-8} (per-site, per-generation). Second, we specified mutation rate and recombination rates of 5×10^{-9} (per-site, per-generation), but the results were qualitatively similar to the results we show. Finally, we considered a mutation rate three times higher in males than in females ($\alpha=3$). We ran simulations in parallel using the Center for High Throughput Computing at the University of Wisconsin-Madison.

Supplementary Material

Supplementary material is available at *Genome Biology and Evolution* online.

Acknowledgments

We thank all members of the Payseur Lab for thoughtful discussions about this work. We additionally thank members of the UW-Madison's Center for High Throughput Computing for providing computational resources and helpful feedback. This work was supported by the

National Institutes of Health (NIH) grant R35GM139412 (to B.A.P.). W.J.S. was partially supported by the NIH Graduate Training Grant in Genetics at the University of Wisconsin-Madison (T32GM007133).

Author Contributions

W.J.S. and B.A.P. designed this study and wrote the manuscript. W.J.S. performed the research with supervision from B.A.P.

Data Availability

The datasets used to produce each figure of this study can be found in [supplementary tables 1 and 2, Supplementary Material](#) online. The computational scripts that were used to generate these data can be found online at: https://github.com/PayseurLabUWMadison/BSR_simulations.

Literature Cited

- Amster G, Sella G. Life history effects on neutral diversity levels of autosomes and sex chromosomes. *Genetics*. 2020;215(4):1133–1142. <https://doi.org/10.1534/genetics.120.303119>.
- Aquadro CF, Begun DJ, Kindahl EC. Selection, recombination, and DNA polymorphism in *Drosophila*. In: Golding B, editor. *Non-neutral evolution: theories and molecular data*. Boston (MA): Springer US; 1994. p. 46–56.
- Avery PJ. The population genetics of haplo-diploids and X-linked genes. *Genet Res*. 1984;44(3):321–341. <https://doi.org/10.1017/S0016672300026550>.
- Baumdicker F, Bisschop G, Goldstein D, Gower G, Ragsdale AP, Tsambos G, Zhu S, Eldon B, Ellerman EC, Galloway JG, et al. Efficient ancestry and mutation simulation with msprime 1.0. *Genetics*. 2022;220(3):iyab229. <https://doi.org/10.1093/genetics/iyab229>.
- Begun DJ, Whitley P. Reduced X-linked nucleotide polymorphism in *Drosophila simulans*. *Proc Natl Acad Sci U S A*. 2000;97(11):5960–5965. <https://doi.org/10.1073/pnas.97.11.5960>.
- Betancourt AJ, Kim Y, Orr HA. A pseudohitchhiking model of X vs. autosomal diversity. *Genetics*. 2004;168(4):2261–2269. <https://doi.org/10.1534/genetics.104.030999>.
- Caballero A. On the effective size of populations with separate sexes, with particular reference to sex-linked genes. *Genetics*. 1995;139(2):1007–1011. <https://doi.org/10.1093/genetics/139.2.1007>.
- Charlesworth B. Background selection and patterns of genetic diversity in *Drosophila melanogaster*. *Genet Res*. 1996;68(2):131–149. <https://doi.org/10.1017/S0016672300034029>.
- Charlesworth B. The effect of life-history and mode of inheritance on neutral genetic variability. *Genet Res*. 2001;77(2):153–166. <https://doi.org/10.1017/S0016672301004979>.
- Charlesworth B, Coyne JA, Barton NH. The relative rates of evolution of sex chromosomes and autosomes. *Am Nat*. 1987;130(1):113–146. <https://doi.org/10.1086/284701>.
- Charlesworth B, Morgan MT, Charlesworth D. The effect of deleterious mutations on neutral molecular variation. *Genetics*. 1993;134(4):1289–1303. <https://doi.org/10.1093/genetics/134.4.1289>.
- Clemente F, Gautier M, Vitalis R. Inferring sex-specific demographic history from SNP data. *PLoS Genet*. 2018;14(1):e1007191. <https://doi.org/10.1371/journal.pgen.1007191>.
- Corl A, Ellegren H. The genomic signature of sexual selection in the genetic diversity of the sex chromosomes and autosomes. *Evolution*. 2012;66(7):2138–2149. <https://doi.org/10.1111/j.1558-5646.2012.01586.x>.
- Crow JF, Denniston C. Inbreeding and variance effective population numbers. *Evolution*. 1988;42(3):482–495. <https://doi.org/10.2307/2409033>.
- Emery LS, Felsenstein J, Akey JM. Estimators of the human effective sex ratio detect sex biases on different timescales. *Am J Hum Genet*. 2010;87(6):848–856. <https://doi.org/10.1016/j.ajhg.2010.10.021>.
- Fernandez-Duque E, Huck M. Till death (or an intruder) do us part: intrasexual-competition in a monogamous primate. *PLoS One*. 2013;8(1):e53724. <https://doi.org/10.1371/journal.pone.0053724>.
- Fu YX. Statistical properties of segregating sites. *Theor Popul Biol*. 1995;48(2):172–197. <https://doi.org/10.1006/tpbi.1995.1025>.
- Goldberg A, Rosenberg NA. Beyond 2/3 and 1/3: the complex signatures of sex-biased admixture on the X chromosome. *Genetics*. 2015;201(1):263–279. <https://doi.org/10.1534/genetics.115.178509>.
- Griffiths RC, Tavaré S. The age of a mutation in a general coalescent tree. *Commun Stat*. 1998;14(1–2):273–295. <https://doi.org/10.1080/15326349808807471>.
- Gutenkunst RN, Hernandez RD, Williamson SH, Bustamante CD. Inferring the joint demographic history of multiple populations from multidimensional SNP frequency data. *PLoS Genet*. 2009;5(10):e1000695. <https://doi.org/10.1371/journal.pgen.1000695>.
- Hammer MF, Mendez FL, Cox MP, Woerner AE, Wall JD. Sex-biased evolutionary forces shape genomic patterns of human diversity. *PLoS Genet*. 2008;4(9):e1000202. <https://doi.org/10.1371/journal.pgen.1000202>.
- Harris M, Kim BY, Garud N. Enrichment of hard sweeps on the X chromosome compared to autosomes in six *Drosophila* species. *Genetics*. 2024;226(4):iyae019. <https://doi.org/10.1093/genetics/iyae019>.
- Hill WG. Effective size of populations with overlapping generations. *Theor Popul Biol*. 1972;3(3):278–289. [https://doi.org/10.1016/0040-5809\(72\)90004-4](https://doi.org/10.1016/0040-5809(72)90004-4).
- Hill WG. Estimation of effective population size from data on linkage disequilibrium. *Genet Res*. 1981;38(3):209–216. <https://doi.org/10.1017/S0016672300020553>.
- Hill WG, Robertson A. Linkage disequilibrium in finite populations. *Theor Appl Genet*. 1968;38(6):226–231. <https://doi.org/10.1007/BF01245622>.
- Huck M, di Fiore A, Fernandez-Duque E. Of apples and oranges? The evolution of “monogamy” in non-human primates. *Front Ecol Evol*. 2020;7(472):1–25. <https://doi.org/10.3389/fevo.2019.00472>.
- Hudson RR. Estimating the recombination parameter of a finite population model without selection. *Genet Res*. 1987;89(5–6):427–432. <https://doi.org/10.1017/S0016672308009610>.
- Hudson RR, Turelli M. Stochasticity overrules the “three-times rule”: genetic drift, genetic draft, and coalescence times for nuclear loci versus mitochondrial DNA. *Evolution*. 2003;57(1):182–190. <https://doi.org/10.1111/j.0014-3820.2003.tb00229.x>.
- Keinan A, Mullikin JC, Patterson N, Reich D. Accelerated genetic drift on chromosome X during the human dispersal out of Africa. *Nat Genet*. 2009;41(1):66–70. <https://doi.org/10.1038/ng.303>.
- Kimura M, Crow JF. The measurement of effective population number. *Evolution*. 1963;17(3):279–288. <https://doi.org/10.2307/2406157>.
- Kirkpatrick M, Guerrero RF, Scarpino SV. Patterns of neutral genetic variation on recombining sex chromosomes. *Genetics*.

- 2010;184(4):1141–1152. <https://doi.org/10.1534/genetics.109.113555>.
- Labuda D, Lefebvre JF, Nadeau P, Roy-Gagnon MH. Female-to-male breeding ratio in modern humans—an analysis based on historical recombinations. *Am J Hum Genet*. 2010;86(3):353–363. <https://doi.org/10.1016/j.ajhg.2010.01.029>.
- Laporte V, Charlesworth B. Effective population size and population subdivision in demographically structured populations. *Genetics*. 2002;162(1):501–519. <https://doi.org/10.1093/genetics/162.1.501>.
- Lawler RR. Monomorphism, male-male competition, and mechanisms of sexual dimorphism. *J Hum Evol*. 2009;57(3):321–325. <https://doi.org/10.1016/j.jhevol.2009.07.001>.
- Lohmueller KE, Bustamante CD, Clark AG. Methods for human demographic inference using haplotype patterns from genomewide single-nucleotide polymorphism data. *Genetics*. 2009;182(1):217–231. <https://doi.org/10.1534/genetics.108.099275>.
- Lohmueller KE, Degenhardt JD, Keinan A. Sex-averaged recombination and mutation rates on the X chromosome: a comment on Labuda et al. *Am J Hum Genet*. 2010;86(6):978–980. <https://doi.org/10.1016/j.ajhg.2010.03.021>.
- Miyata T, Hayashida H, Kuma K, Mitsuyasu K, Yasunaga T. Male-driven molecular evolution: a model and nucleotide sequence analysis. *Cold Spring Harb Symp Quant Biol*. 1987;52:863–867. <https://doi.org/10.1101/SQB.1987.052.01.094>.
- Musharoff S, Shringarpure S, Bustamante CD, Ramachandran S. The inference of sex-biased human demography from whole-genome data. *PLoS Genet*. 2019;15(9):e1008293. <https://doi.org/10.1371/journal.pgen.1008293>.
- Palamara PF, Lencz T, Darvasi A, Pe'er I. Length distributions of identity by descent reveal fine-scale demographic history. *Am J Hum Genet*. 2012;91(5):809–822. <https://doi.org/10.1016/j.ajhg.2012.08.030>.
- Pool JE, Nielsen R. Population size changes reshape genomic patterns of diversity. *Evolution*. 2007;61(12):3001–3006. <https://doi.org/10.1111/j.1558-5646.2007.00238.x>.
- Santiago E, Novo I, Pardiñas AF, Saura M, Wang J, Caballero A. Recent demographic history inferred by high-resolution analysis of linkage disequilibrium. *Mol Biol Evol*. 2020;37(12):3642–3653. <https://doi.org/10.1093/molbev/msaa169>.
- Tajima F. Evolutionary relationship of DNA sequences in finite populations. *Genetics*. 1983;105(2):437–460. <https://doi.org/10.1093/genetics/105.2.437>.
- Tajima F. The effect of change in population size on DNA polymorphism. *Genetics*. 1989;123(3):597–601. <https://doi.org/10.1093/genetics/123.3.597>.
- Veeramah KR, Gutenkunst RN, Woerner AE, Watkins JC, Hammer MF. Evidence for increased levels of positive and negative selection on the X chromosome versus autosomes in humans. *Mol Biol Evol*. 2014;31(9):2267–2282. <https://doi.org/10.1093/molbev/msu166>.
- Vicoso B, Charlesworth B. Effective population size and the faster-X effect: an extended model. *Evolution*. 2009;63(9):2413–2426. <https://doi.org/10.1111/j.1558-5646.2009.00719.x>.
- Wall JD, Andolfatto P, Przeworski M. Testing models of selection and demography in *Drosophila simulans*. *Genetics*. 2002;162(1):203–216. <https://doi.org/10.1093/genetics/162.1.203>.
- Waples RS. A bias correction for estimates of effective population size based on linkage disequilibrium at unlinked gene loci. *Conserv Genet*. 2006;7(2):167–184. <https://doi.org/10.1007/s10592-005-9100-y>.
- Waples RS. What is N_e , anyway? *J Hered*. 2022;113(4):371–379. <https://doi.org/10.1093/jhered/esac023>.
- Watterson GA. On the number of segregating sites in genetical models without recombination. *Theor Popul Biol*. 1975;27(2):256–276. [https://doi.org/10.1016/0040-5809\(75\)90020-9](https://doi.org/10.1016/0040-5809(75)90020-9).
- Webster TH, Wilson Sayres MA. Genomic signatures of sex-biased demography: progress and prospects. *Curr Opin Genet Dev*. 2016;41:62–71. <https://doi.org/10.1016/j.gde.2016.08.002>.
- Wright S. Inbreeding and homozygosity. *Proc Natl Acad Sci U S A*. 1933;19(4):411–420. <https://doi.org/10.1073/pnas.19.4.411>.
- Wright S. Breeding structure of populations in relation to speciation. *Am Nat*. 1940;74(752):232–248. <https://doi.org/10.1086/280891>.

Associate editor: Andrea Betancourt